In-vivo cancer cell destruction using porous silicon nanoparticles

Chanseok Hong[a], Jungkeun Lee[a], Mikwon Son[b], Soon Sun Hong[b] and Chongmu Lee[a]

In-vivo animal tests were performed to investigate the feasibility of photothermal therapy based on porous silicon nanoparticles (PSiNPs) in combination with a near-infrared (NIR) laser. The in-vivo animal test results showed that the murine colon carcinoma (CT-26) tumors were completely resorbed with minimal damage to surrounding healthy tissue within 5 days after PSiNPs and NIR laser treatments. In contrast, tumors in the groups treated only with PSiNPs or NIR and a control group continued to grow until the mice died. All of the mice treated with both PSiNPs and NIR remained healthy and free of tumors even 90 days after the treatment. In-vivo fluorescence imaging and the urine and feces tests revealed that PSiNPs injected intratumorally into mice were cleared mainly through the urine. The in-vivo animal test results suggest that thermotherapy based on porous silicon in combination with NIR laser irradiation can efficiently destroy cancer cells selectively without damaging the surrounding healthy cells. *Anti-Cancer Drugs* 22:971–977 © 2011 Wolters Kluwer Health | Lippincott Williams & Wilkins.

Anti-Cancer Drugs 2011, **22**:971–977

Keywords: cancer therapy, in-vivo animal test, near-infrared laser, porous silicon, urine test

[a]Department of Materials Science and Engineering and [b]College of Medicine, Inha University, Incheon, Korea

Correspondence to Chongmu Lee, PhD, Department of Materials Science and Engineering, Inha University, Incheon, Korea
Tel: +82 32 860 7536; fax: +82 32 860 5546;
e-mail: cmlee@inha.ac.kr

Received 6 July 2011 **Revised form accepted** 2 August 2011

Introduction

Inorganic nanomaterials such as gold nanoparticles [1–10], gold nanorods [11–14], gold nanoshells [15–19], gold nanocages [20,21], gold nanocrystals [22,23], and single-wall carbon nanotubes [24–26], porous silicon nanoparticles (PSiNPs) [27,28], and TiO_2 nanotubes [29,30] have been shown to act as thermal coupling agents in photothermotherapies (PTTs) by many investigators. PSiNPs, however, have not been investigated extensively despite their attractive properties for the treatment of cancer. PSiNPs possess a number of properties that make them attractive for biological applications including good biocompatibility [31] and biodegradability [32], a tunable nanostructure for drug delivery [33], excellent photothermal properties [28], and a readily functionalized surface [34]. Since the first in-vivo use of porous silicon (PSi), anticancer therapeutics based on PSiNPs have been widely studied [27,28,35–39].

Cancer treatments using PSi can be carried out in many ways. One method is drug delivery. PSiNPs loaded with drugs such as cisplatin and doxorubicin have been demonstrated to destroy cancer cells successfully [35,36]. Another technique is photodynamic therapy. PSiNPs in combination with near-infrared (NIR) light irradiation have been shown to produce singlet oxygen for tumor cell destruction [37–39]. A third method is PTT. PSiNPs combined with NIR have exhibited the ability to cause photothermal damage in tumor cells [27,28]. In particular, there are few reports on the PPT using PSiNPs despite their excellent photothermal properties and their attractive properties related to their in-vivo use as above. We reported previously on the excellent heat-generating ability of PSiNPs and their ability to destroy cancer cells irreversibly under NIR laser irradiation as noted in the temperature rise measurement and MTT assay results, respectively [27,28]. In this study, we report the in-vivo animal test results of PSiNPs in combination with an NIR laser to investigate the ability of PSiNPs to kill cancer cells, their ability to inhibit the growth of tumors and the clearance of PSiNPs through urination after the laser treatments.

Materials and methods

Preparation of PSiNPs/EtOH : polyethyleneglycol drug solutions

First, PSi layers were prepared on $2.5 \times 2.5 \times 0.05$ cm pieces of p-type Si(100) with a resistivity of 5–10 Ωcm by anodic etching in a 1 : 1 (by volume) solution of 46% HF and 95% C_2H_5OH at a current density of 200 mA/cm^2 for 150 s. This set of etching process parameters was used to form meso-PSi (2 nm < pore size < 50 nm). The porosity and thickness of the PSi layers as determined by weight measurements [40] were approximately 73% and 55 μm, respectively. The details of the anodization process have been described in the literature [27]. The PSi layers formed on Si(100) were then lifted off by anodic etching in a 1 : 15 (by volume) solution of 46% HF and 95% C_2H_5OH at a current density of 4 mA/cm^2 for 250 s. The free-standing PSi layers were then fractured into PSiNPs by ultrasonication in 10 ml of ethanol for 24 h. The PSiNPs were subsequently filtered twice first with a 450 nm membrane and then with a 220 nm membrane. PSiNPs/EtOH : polyethyleneglycol

0959-4973 © 2011 Wolters Kluwer Health | Lippincott Williams & Wilkins DOI: 10.1097/CAD.0b013e32834b859c

(PEG) drug solutions were prepared by dispersing the resulting PSiNPs in 10 ml of ethanol mixed with 10 ml of thiolated polyethyleneglycol (PEG-SH) and these were centrifuged for 24 h until all of the PSi particles were dispersed.

Cells and materials

The murine colon cancer cell lines (CT-26) were purchased from the Korean Cell Line Bank (KCLB, Seoul, Korea). CT-26 cells were cultured in Dulbecco's modified Eagle's medium, supplemented with 10% fetal bovine serum and 1% penicillin/streptomycin. The fetal bovine serum, cell culture media, penicillin-streptomycin, and all of the other agents used in the cell culture studies were purchased from Invitrogen (GIBCO, New York, USA). The cultures were maintained at 37°C in a CO_2 incubator under a controlled humidified atmosphere composed of 95% air and 5% CO_2. Trypan blue dyes were purchased from Sigma-Aldrich (St. Louis, Missouri, USA).

In-vivo animal tests

Animal care and all experimental procedures pertaining to animals were conducted in accordance with the Guide for Animal Experiments edited by the Korean Academy of Medical Sciences. The CT-26 cells (1×10^6 cells) were suspended in 100 µl PBS and were subcutaneously injected into the backs of male mice of each group ($n = 5$, 5–6 weeks old, Balb/c). When the tumors had grown to a volume of 65–70 mm^3, the mice were randomly placed into five groups: (a) mice were simply monitored without any other treatment; (b) mice were intratumorally injected with 100 µl of PBS and then irradiated with a NIR laser three times at 1.5 W/cm^2 for 2 min each time at a time interval of 1 min under ether anesthesia; (c) mice were intratumorally injected with a PSiNPs/EtOH : PEG solution (0.7 g/l, 100 µl) without NIR laser irradiation; (d) mice were injected with PSiNPs/EtOH : PEG (0.7 g/l, 100 µl) into the tumor, followed by immediate irradiation by an NIR laser at 1.5 W/cm^2 on the tumor region in the same manner as in (a); and (e) mice were injected with PSiNPs/EtOH : PEG (0.7 g/l, 100 µl) into the tumor, followed by immediate irradiation with an NIR laser at 0.5 W/cm^2 on the tumor region.

The mice were anesthetized with an injection of 40 µl of a 9 : 1 solution of ketamine (100 mg/ml) and rompun (100 mg/ml). Tumor volumes, animal body weights, and tumor conditions were recorded weekly for the duration of the study [41]. The tumor size of each group was measured using a skinfold caliper, and the tumor volumes were calculated using the following equation: tumor volume = $ab^2/2$, where a is the maximum diameter of the tumor and b is the minimum diameter of the tumor [42]. All of the procedures for in-vivo experiments were performed in accordance with the guidelines of the Department of Biomedical Science, Inha University, with regard to animal care and use.

In-vivo fluorescence imaging studies

Nude mice bearing CT-26 tumors were injected intramuscularly and with a dose of PSiNPs/EtOH : PEG (0.7 g/l, 300 nmol/l in 20 µl PBS) and irradiated with NIR. They were then imaged with GFP excitation (445–490 nm) and an ICG (810–875 nm) emission filter using an IVIS 200 imaging system 24 and 72 h after the injection.

Fig. 1

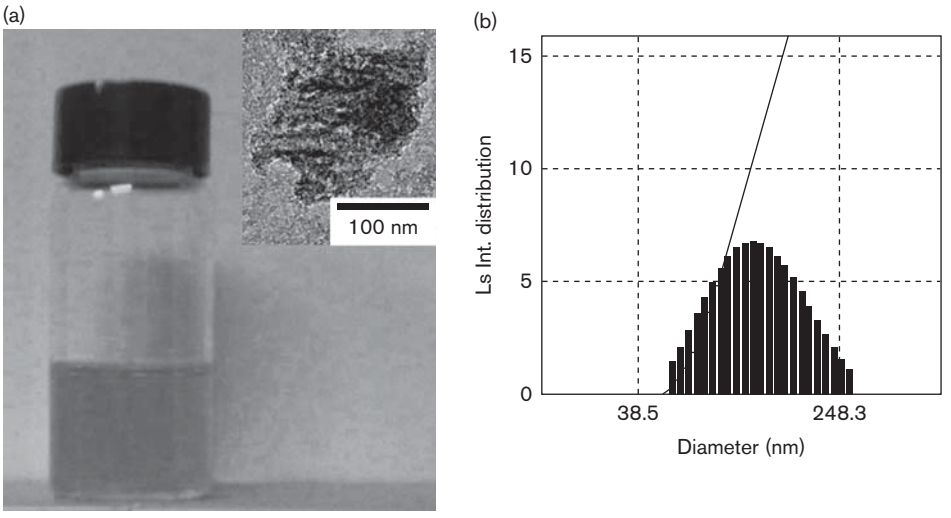

Porous silicon (PSi) particle size distribution: (a) PSi/EtOH : polyethyleneglycol (PEG) solution and (b) the distribution of the diameters of PSi nanoparticles in the PSi/EtOH : PEG solution. (Light scattering intensity distribution).

Results

Size distribution of the PSiNPs in the PSi/EtOH : PEG solution

The PSiNPs functionalized with PEG were well solubilized and therefore became uniformly distributed in the PSiNPs/EtOH : PEG solution without forming any floating particles, precipitates, or agglomerates for a long period of time as shown Fig. 1a. Each PSi particle in the solution contained many nanopores with a size of a few to a few tens of nanometers (inset in Fig. 1a). Functionalization of PSiNPs with PEG is necessary to enhance the internalization of PSiNPs into cells as well as the attachment of antibodies to PSiNPs for the systematic administration of cancer. Ethyl alcohol was also used to enhance the dispersion of PSiNPs in the solution. Figure 1b displays the size distribution of the PSiNPs after they were filtered using a 220 nm membrane. They ranged in size from 51–267 nm, with an average diameter of approximately 105 nm. The existence of PSiNPs larger than 220 nm is presumably because of the local tearing of the membrane that occurred during the filtering process. Hence, needle-like PSiNPs longer than 220 nm were included in the solution at 4.7f(1s)%, (the fraction of the light scattering by the electrons in the 1s orbital of the Si atoms in the nanoparicles with a diameter larger than 220 nm to that by the electrons in the 1s orbital of the Si atoms in total nanoparticles).

In-vivo animal tests

In-vivo therapeutic examinations were attempted with Balb/c mice bearing CT-26 tumors grown on their backs

Fig. 2

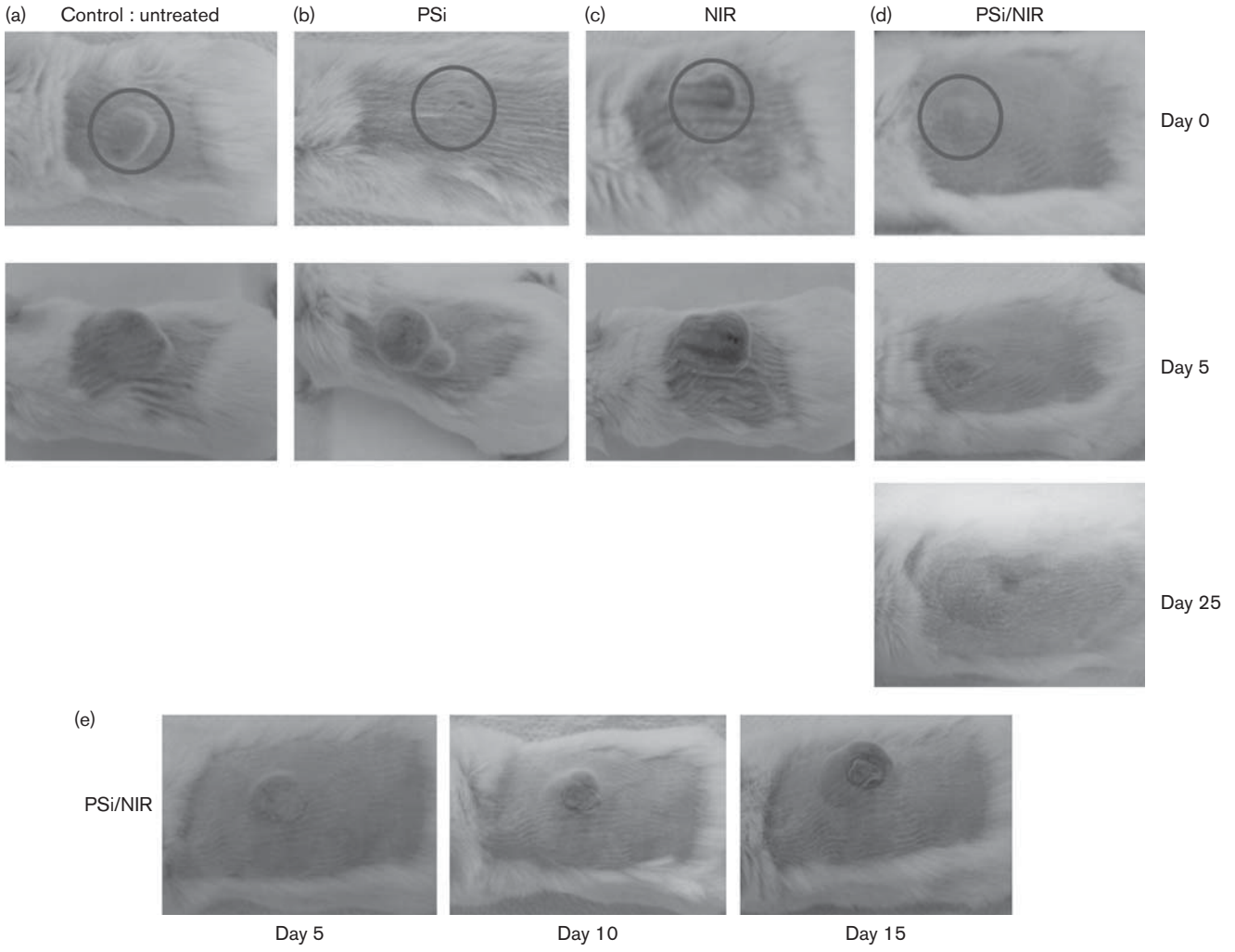

In-vivo animal test results. Photographs of the tumors of the mice treated differently 24 h after treatment: (a) neither porous silicon nanoparticles (PSiNPs) nor a laser treatment (control), (b) PSiNPs treatment only, (c) near-infrared (NIR) laser treatment only (NIR laser irradiation three times for 2 min at 1.5 W/cm^2 each time at a time interval of 2 min), (d) PSiNPs treatment [porous silicon (PSi) concentration = 0.7 g/l], followed by laser treatment (NIR laser irradiation three times for 2 min at 1.5 W/cm^2 each time at a time interval of 1 min), and (e) PSiNPs treatment (PSi concentration = 0.7 g/l), followed by laser treatment (NIR laser irradiation three times for 2 min at 0.5 W/cm^2 each time at a time interval of 1 min).

to confirm that the photothermal effect of PSiNPs combined with the NIR laser could efficiently destroy tumor cells without causing damage to any of the surrounding healthy cells. When the tumors had grown to a volume of ~100 mm^3, PSiNPs/EtOH : PEG solution (0.7 g/l, 100 µl) was then injected directly into the tumor regions. Mice ready for irradiation were placed under a focal lens through which the NIR laser could be focused to have a power density of 0.5 or 1.5 W/cm^2. They were then irradiated three times for 2 min each time at a time interval of 1 min. This intermittent laser irradiation was designed to minimize the damage of the healthy tissues adjacent to the tumor tissues.

We investigated the tumor volume changes in mice subjected to different treatments as follows: (Group 1) a control group without any treatment; (Group 2) a group treated only with PSiNPs; (Group 3) a group treated only with an NIR laser; (Group 4) a group treated with both PSiNPs and the NIR laser (1.5 W/cm^2); and (Group 5) a group treated with both PSiNPs and the NIR laser (0.5 W/cm^2). The control group (Group 1) and the group treated only with PSiNPs (Group 2) or the NIR laser (Group 3) showed considerable growth of the tumors 5 days after the treatment. All of the mice in these groups died within 20 days because of the significant growth of the tumors without exception Fig. 2a–c. In contrast, in Group 4, laser treatment at a higher irradiation intensity (1.5 W/cm^2) led to complete necrosis of their tumors 5 days after the treatments and complete recovery 25 days after the treatment, with the regrowth of fur on the original tumor site (Fig. 2d). The tumor seemed to have already shrunk to a nearly zero volume at day 5 posttreatment. In contrast, in Group 5, treated with a lower irradiation intensity (0.5 W/cm^2), the tumors once stopped growing (5 days after the treatment) and then decreased in size to some degree (10 days after the treatment), but regrew (15 days after the treatment) until the mice died (about 20 days after the treatment, Fig. 2e). The recurrence of a tumor despite a laser beam diameter (1.5 cm) large enough to cover the entire tumor area may have been because of the insufficient heat generated by the PSiNPs during the NIR laser irradiation process at 0.5 W/cm^2. This insufficient thermal budget failed to destroy all of the tumor cells, resulting in the regrowth of the tumors.

These observations revealed that only a combination of PSiNPs and laser treatments with a sufficiently high irradiation intensity resulted in the complete destruction of tumors. It is important to note that the mice in Group 4 remained healthy without any side effects such as abnormal growth or recurrence of their tumors for more than 3 months. We found the results highly reproducible, obtaining similar results for the experiments conducted in triplicate. Figure 3 presents the tumor growth rates of the five groups subjected to different treatments. Only Group 4 exhibited almost no change in the tumor volume,

Fig. 3

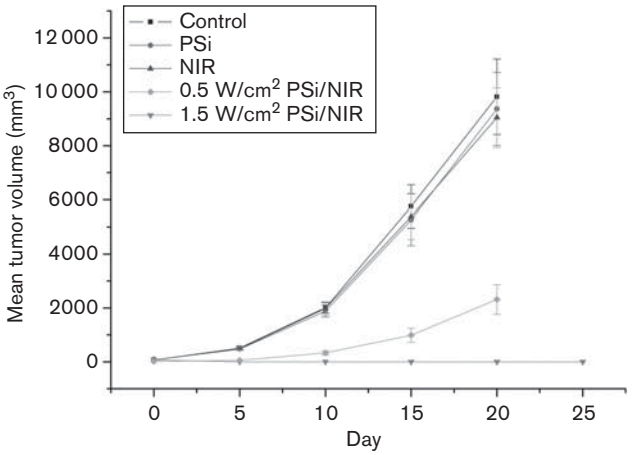

Tumor volume as a function of time after photothermal treatments. Tumor volume of CT-26 tumor cell xenografts. Tumor volumes were measured once a week after the sample treatments. The group treated with a porous silicon (PSi)/EtOH : polyethyleneglycol solution, followed by near-infrared (NIR) laser treatments (four times for 1 min at 1.5 W/cm^2 each time at a time interval of 2 min) showed efficient tumor growth inhibition compared with the other experimental groups.

whereas the other groups showed continuous tumor growth until they died approximately 15 days after the treatments.

Weight change after laser treatment

One of the most important issues in PTT using inorganic nanomaterials is the toxicity of the nanomaterials to the organs of the human body. The toxicity of PSiNPs to the organs of mice was examined indirectly by measuring the change in the weights after the laser treatment. It is widely accepted that the animals subjected to toxic treatments lose weight. The average body weight of the mice before the photothermal treatment was 26.0 g whereas that of a control group (normal mice without any tumor) was 25.1 g. The weights of the mice treated with PSiNPs, followed by a laser treatment increased slightly in a pattern similar to that noted in the normal mice without tumors Fig. 4, indicating that the mice continued to mature without any significant toxic effect.

Renal clearance of PSiNPs

Another important issue is that the inorganic nanomaterials used *in vivo* are removed renally within a reasonable period of time. According to previous reports, silicon is a common trace element in human bodies. A biodegradation product of PSi, orthosilicic acid ($Si(OH)_4$), is the form most easily absorbed by humans. It is also found in numerous tissues. Furthermore, silicic acid administered to humans is efficiently excreted through the urine. Park *et al.* [43] reported that the PSi nanoparticles accumulated

Fig. 4

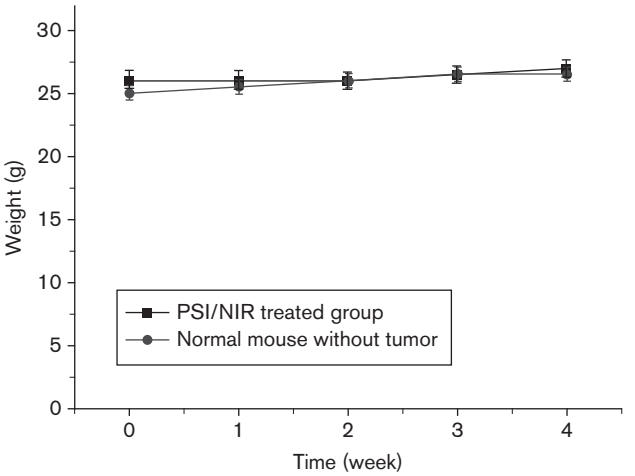

Change in body weight of mice. Change in the body weight of the mice injected with a porous silicon (PSi)/EtOH : polyethyleneglycol solution, followed by near-infrared (NIR) laser treatments (four times for 1 min at 1.5 W/cm^2 each time at a time interval of 1 min). There was no significant body weight loss for apparent side effects.

in the organs are noticeably cleared from the body within a period of 1 week and completely cleared in 4 weeks. To investigate the removal of PSiNPs from an organism, urine and feces tests were conducted. Figure 5a compares the amounts of silicon in the urine and feces of the group treated with PSiNPs and the NIR laser with those of the control group (untreated). The amount of PSiNPs in the urine of the PSiNPs-treated group was found to be nearly about three times higher than that of the control. In contrast, there was no noticeable difference in the amount of silicon in the feces between the two groups. In-vivo fluorescence images of the PSiNPs injected intratumorally into a mouse showed that the density of Si in the bladder was lower 72 h after the injection (Fig. 5c) compared with the level 24 h after the injection (Fig. 5b). These results verify that PSiNPs injected intratumorally into mice are cleared mainly through the urine.

Discussion

An in-vitro cell test and in-vivo animal test were performed to investigate the feasibility of the photothermal therapy based on PSiNPs in combination with a

Fig. 5

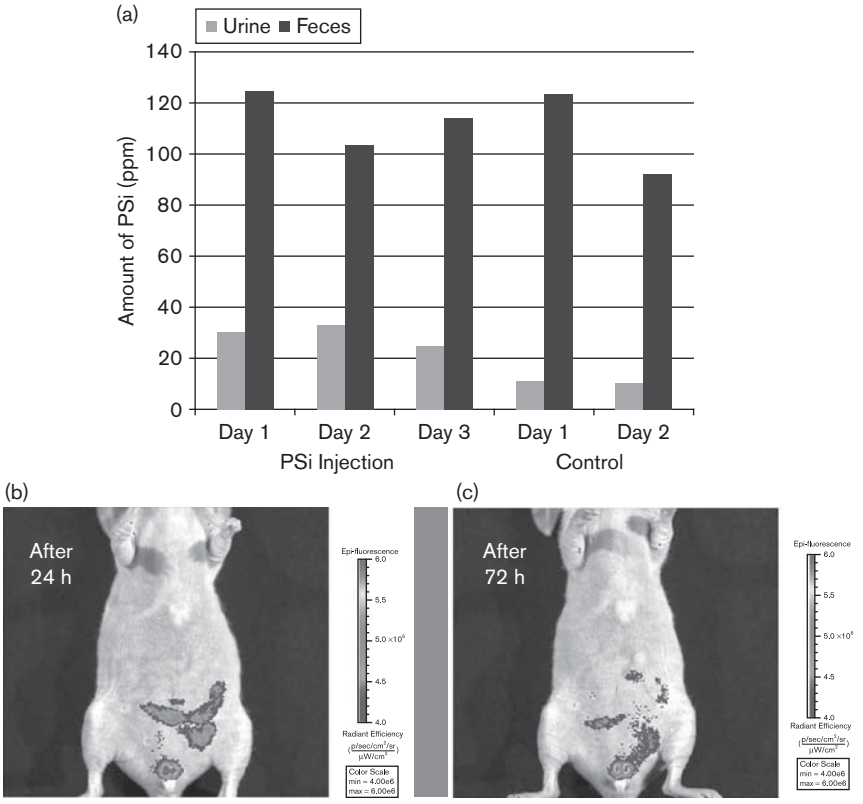

Clearance of porous silicon nanoparticles (PSiNPs) through the urine and feces: (a) comparison of the amounts of PSiNPs in the urine and feces between the group treated with porous silicon (PSi) and an untreated control group, and in-vivo fluorescence images of PSiNPs after 24 h (b) and 72 h (c).

NIR laser. A combination of PSiNPs and NIR laser treatment techniques showed a substantially higher cell death rate compared with the use of only one of these two techniques. The murine colon carcinoma (CT-26) tumors were completely resorbed without causing much damage to the surrounding healthy tissue within 5 days of the PSiNPs and NIR laser treatment. All of the mice given both treatments remained healthy and free of tumors and side effects for more than 3 months. The weights of the mice treated with PSiNPs, followed by a laser treatment increased slightly in a pattern similar to that noted in the normal mice without tumors, indicating that the mice continued to mature without any significant toxic effect. The preliminary results presented in this work show the feasibility of PPT based on PSiNPs in combination with NIR laser irradiation in selectively destroying cancer cells without damaging the surrounding healthy cells. However, the systematic administration of cancers still remains a challenge in this therapeutic approach. Experiments to access this are under way using tumor-targeting techniques such as functionalization of PSiNPs with specific antibodies.

Acknowledgements

This study was financially supported by the Korean Science and Engineering Foundation (KOSEF) through the 2010 Core Research Program.

Conflicts of Interest

There are no conflicts of interest.

References

1 Pitsillides CM, Joe EK, Wei X, Anderson RR, Lin CP. Selective cell targeting with light-absorbing microparticles and nanoparticles. *Biophys J* 2003; **84**:4023–4032.
2 Zharov VP, Galitovskaya V, Viegas M. Photothermal detection of local thermal effects during selective nanophotothermolysis. *App Phys Lett* 2003; **83**:4897–4899.
3 Zharov VP, Galitovskaya EN, Viegas M. Photothermal guidance for selective photothermolysis with nanoparticles. *Proc SPIE* 2004; **5319**:291–300.
4 Hainfeld JF, Slatkin DN, Smilowitz HM. The use of gold nanoparticles to enhance radiotherapy in mice. *Phys Med Biol* 2004; **49**:N309–N315.
5 Zharov VP, Galitovskaya EN, Johnson C, Kelly T. Synergistic enhancement of selective nanophoto thermolysis with gold nanoclusters: potential for cancer therapy. *Lasers Surg Med* 2005; **37**:219–226.
6 El-Sayed IH, Huang X, El-Sayed MA. Selective laser photo-thermal therapy of epithelial carcinoma using anti-EGFR antibody conjugated gold nanoparticles. *Cancer Lett* 2006; **239**:129–135.
7 Huang X, Jain PK, El-Sayed IH, El-Sayed MA. Determination of the minimum temperature required for selective photothermal destruction of cancer cells using immunotargeted gold nanoparticles. *Photochem Photobiol* 2006; **82**:412–417.
8 Khlebtsov B, Zharov V, Melnikov A, Tuchin V, Khlebtsov N. Optical amplification of photothermal therapy with gold nanoparticles and nanoclusters. *Nanotechnology* 2006; **17**:5167–5179.
9 Terentyuk GS, Maslyakova GN, Suleymanova LV, Khlebtsov NG, Khlebtsov BN, Akchurin GG, *et al.* Laser-induced tissue hyperthermia mediated by gold nanoparticles: toward cancer phototherapy. *J Biomed Opt* 2009; **14**:021016–021018.
10 Terentyuk GS, Maslyakova GN, Suleymanova LV, Khlebtsov BN, Kogan BY, Akchurin GG, *et al.* Circulation and distribution of gold nanoparticles and induced alterations of tissue morphology at intravenous particle delivery. *J Biophoton* 2009; **2**:292–302.
11 Huang X, El-Sayed IH, El-Sayed MA. Cancer cell imaging and photothermal therapy in the near-infrared region by using gold nanorods. *J Am Chem Soc* 2006; **128**:2115–2120.
12 Takahashi H, Niidome T, Nariai A, Niidome T, Yamada S. Gold nanorod-sensitized cell death: Microscopic observation of single living cells irradiated by pulsed near-infrared laser light in the presence of gold nanorods. *Chem Lett* 2006; **35**:500–501.
13 Takahashi H, Niidome T, Nariai A, Niidome Y, Yamada S. Photothermal reshaping of gold nanorods prevents further cell death. *Nanotechnology* 2006; **17**:4431–4435.
14 Huff TB, Tong L, Zhao Y, Hansen MN, Cheng JK, Wei A. Hyperthermic effects of gold nanorods on tumor cells. *Nanomedicine* 2007; **2**:125–132.
15 Hirsch LR, Stafford RL, Baukson JA, Sershen SR, Rivera B, Price RE, *et al.* Nanoshell-mediated near-infrared thermal therapy of tumors under magnetic resonance guidance. *Proc Natl Acad Sci USA* 2003; **100**:13549–13554.
16 Jordan A, Maier-Hauff K, Wust P, Johaunsen M. Nanoparticles for thermotherapy. In: Kumar C, editor. *Nanomaterials for cancer therapy.* Weinheim: Wiley-VCH. 2006; pp. 242–258. and references therein.
17 Loo C, Lin A, Hirsch L, Lee MH, Barton J, Halas N, *et al.* Nanoshell-enabled photonics-based imaging and therapy of cancer. *Tech Cancer Res Treat* 2004; **3**:33–40.
18 O'Neal DP, Hirsch LR, Halas NJ, Payne JD, West JL. Photothermal tumor ablation in mice using near infrared absorbing nanoshells. *Cancer Lett* 2004; **209**:171–176.
19 Loo C, Lowery A, Halas NJ, West JL, Drezek R. Immunotargeted nanoshells for integrated cancer imaging and therapy. *Nano Lett* 2005; **5**:709–711.
20 Chen J, Wiley B, Li ZY, Campbell D, Saeki F, Cang H, *et al.* Gold nanocages: engineering their structure for biomedical applications. *Adv Mater* 2005; **17**:2255–2261.
21 Hu M, Petrova H, Chen J, McLellan JM, Siekkinen AR, Marquez M, *et al.* Ultrafast laser studies of the photothermal properties of gold nanocages. *J Phys Chem B* 2006; **110**:1520–1524.
22 Link S, El-Sayed MA. Shape and size dependence of radiative, non-radiative and photothermal properties of gold nanocrystals. *Int Rev Phys Chem* 2000; **19**:409–453.
23 Link S, El-Sayed MA. Optical properties and ultrafast dynamics of metallic nanocrystals. *Ann Rev Phys Chem* 2003; **54**:331–366.
24 Kam NWS, O'Connell M, Wisdom JA, Dai H. Carbon nanotubes as multifunctional biological transporters and near-infrared agents for selective cancer cell destruction. *Proc Natl Acad Sci USA* 2005; **102**: 11600–11605.
25 Zavaleta C, De la Zerda A, Liu Z, Keren S, Cheng Z, Schipper M, *et al.* Noninvasive Raman spectroscopy in living mice for evaluation of tumor targeting with carbon nanotubes. *Nano Lett* 2005; **8**:2800–2805.
26 Panchapakesan B, Lu S, Sivakumar K, Taker K, Cesarone G, Wickstrom E. Single-wall carbon nanotube nanobomb agents for killing breast cancer cells. *Nanobiotechnology* 2005; **1**:133–139.
27 Lee C, Kim H, Cho Y, Lee WI. The properties of porous silicon as a therapeutic agent via the new photodynamic therapy. *J Mater Chem* 2007; **17**:2648–2653.
28 Lee C, Kim H, Hong C, Kim M, Hong SS, Lee DH, *et al.* Porous silicon as an agent for cancer thermotherapy based on near-infrared light irradiation. *J Mater Chem* 2008; **18**:4790–4795.
29 Lee C, Hong C, Kim H, Kang J, Zheng HM. TiO_2 nanotubes as a therapeutic agent for cancer thermotherapy. *Photochem Photobiol* 2010; **86**:981–989.
30 Hong C, Kang J, Lee J, Zheng HM, Hong S, Lee D, *et al.* Photothermal therapy using TiO_2 nanotubes in combination with near-infrared laser. *J Cancer Ther* 2010; **1**:52–58.
31 Bayliss SC, Heald R, Fletcher DI, Buckberry LD. The culture of mammalian cells on nanostructured silicon. *Adv Mater* 1999; **11**:318–321.
32 Canham LT. Bioactive silicon structure fabrication through nanoetching techniques. *Adv Mater* 1995; **7**:1033–1037.
33 Salonen J, Kaukonen AM, Hirvonen J, Lehto VP. Mesoporous silicon in drug delivery applications. *J Pharm Sci* 2008; **97**:632–653.
34 Anglin EJ, Cheng L, Freeman WR. Sailor MJ. Porous silicon in drug delivery devices and materials. *Adv Drug Delivery Rev* 2008; **60**: 1266–1277.
35 Li X, Coffer JL, Chen Y, Pinizzotto RF, Newey J, Canham LT. Transition metal complex-doped hydroxyapatite layers on porous silicon. *J Am Chem Soc* 1998; **120**:11706–11709.
36 Vaccari L, Canton D, Zaffaroni N, Villa R, Tormen M, Di Fabrizio E. Porous silicon as drug carrier for controlled delivery of doxorubicin anticancer agent. *Microelectron Eng* 2006; **83**:1598–1601.

37 Parkhutik V, Chirvony V, Matveyeva E. Optical properties of porphyrin molecules immobilized in nano-porous silicon. *Biomol Eng* 2007; **24**:71–73.
38 Schmidt R. Photosensitized generation of singlet oxygen. *Photochem Photobiol* 2006; **82**:1161–1177.
39 Chirvony V, Bolotin V, Matveeva E, Parkhutik V. Fluorescence and O-1(2) generation properties of porphyrin molecules immobilized in oxidized nanoporous silicon matrix. *J Photochem Photobiol A* 2006; **181**:106–113.
40 Halimaoui A. Lecture 3, Porous silicon: material processing, properties and applications. In: Vial J-C, Derrien J, editors. *Porous silicon science and technology*. Berlin and Heidelberg: Springer-Verlag; 1995.
41 Azrak RG, Frank CL, Ling X, Slocum HK, Li F, Foster BA, *et al.* The mechanism of methylselenocysteine and docetaxel synergistic activity in prostate cancer cells. *Mol Cancer Ther* 2006; **5**: 2540–2548.
42 Yao YM, Liu QG, Yang W, Zhang M, Ma QY, Pan CE. Effect of spleen on immune function of rats with liver cancer complicated by liver cirrhosis. *Hepatobiliary Pancreat Dis Int* 2003; **2**:242–246.
43 Park JH, Gu L, Von Maltzahn G, Ruoslahti E, Bhatia SN, Sailor M. Biodegradable luminescent porous silicon nanoparticles for *in vivo* applications. *Nat Mater* 2009; **8**:331–336.